INTERNATIONAL DESIGN CONFERENCE – DESIGN 2022
https://doi.org/10.1017/pds.2022.62

Effect of Heat Treatment on the Hardness of Unconventional Geometrical Features for Laser Powder Bed Fused AlSi10Mg

L. Strauß [1], J. Montero [2], S. Weber [1,✉], S. Brenner [1], P. Höfer [1], K. Paetzold [2] and G. Löwisch [1]

[1] Universität der Bundeswehr München, Germany, [2] Technische Universität Dresden, Germany

✉ s.weber@unibw.de

Abstract

The adoption of Design for Additive Manufacturing (DfAM) practices brought new industrial components embedding unconventional shapes such as lattice structures or freeform surfaces resulting from topological optimisations. As a drawback of design freedom, designers need to use thermal post-processing to achieve homogeneous properties in metal 3D printing. This contribution analyses the effect of T6-like heat treatment on the hardness of a complex component. Hardness values are reported along with good design practices for effective thermal post-processing to complement the DfAM knowledge base.

Keywords: additive manufacturing, 3D printing, design for x (DfX), heat treatment, hardness

1. Introduction

Metallic 3D printing or additive manufacturing (AM) processes like laser-based powder bed fusion (PBF-LB) allow designers to create new geometries, enabling more significant design freedom than conventional manufacturing (CM) processes (Thompson et al., 2016). Therefore, AM introduces new constraints and possibilities, studied by Design for AM (DfAM) approaches (Vaneker et al., 2020). These approaches aid designers in the different design stages to reach optimal solutions. For example, DfAM heuristics, principles, and guidelines give recommendations for the conceptual and embodiment design phases (Schmitt et al., 2020). Most of them encourage designers to use a large amount of complexity, as it comes almost at no expense (Kirchheim et al., 2017), and unconventional geometries like topology optimised bodies and surfaces or lattice structures (Brackett et al., 2011).
The way the AM process operates alters the mechanical properties of PBF-LB parts with such complex geometries. As the process involves solidification on a layer-basis and a moving heat source, which subjects the parts to a cyclic thermal load, AM leads to anisotropic properties in the as-built condition (Kok et al., 2018). This anisotropy depends on the material and geometry and may severely affect geometries like lattice structures. Therefore, thermal post-processing is recommended to diminish these effects. The aluminium alloy AlSi10Mg is a widely used material for PBF-LB metal parts due to its good properties like high strength, good fatigue life, low density, and cost. Yet, the PBF-LB of AlSi10Mg leads to a fine microstructure, which results in high strength and low fracture strain. In addition, residual stress occurs due to the inhomogeneous distribution of properties (Read et al., 2015). These characteristics combined with process-related emerged pores and the brittleness of AlSi10Mg lead to low fatigue strength and therefore low persistence. These drawbacks can be improved by using thermal post-processing like the widespread T6 heat treatment, which is preferred for high strength applications in contrast to T5 that offers higher ductility (Schuch et al., 2021).

https://doi.org/10.1017/pds.2022.62 Published online by Cambridge University Press

There are just a few studies, which deal with the analysis of effects of heat treatment on unconventional AM geometries (Liu et al., 2020a), but none that targets design recommendations using an actual industrial application. For these reasons, this article presents an automotive case study for an additive manufactured AlSi10Mg part with unconventional features. Furthermore, most PBF-LB parts need support structures that attach the part to the build platform and help to mitigate build failure induced by part deformation and residual stresses (Cheng et al., 2019; Cloots et al., 2013). The support structures are a barrier to the heat treatment and might affect its effectivity significantly, as thermal post-processing is usually performed before support removal. Therefore, this contribution investigates the heat treatment and its effects on the hardness of a 3D printed industrial component that infers unfavourable conditions for heat treatment. These unfavourable conditions include a varying wall thickness, as well as a large amount of support structure. In detail, this means that the short heat treatment period relative to the wall thickness might lead to an insufficient temperature increase on the inside. In addition, a higher wall thickness and a high density of support structures can have an undesirable effect on the quenching, which further leads to poor and inhomogeneous characteristics. The exposed research gaps lead to the following research questions:

- RQ1: How does thermal post-processing affect the mechanical properties and particularly the hardness of DfAM features in an industrial AM part?
- RQ2: How can designers take advantage and exploit DfAM knowledge on thermal post-processing?

The article is organized into five sections. Following this introduction, a literature review is provided as the state-of-the-art section. The current practices for heat treatment of laser powder bed fused AlSi10Mg and their effect on mechanical properties are presented. Furthermore, existing studies on the impact of heat treatment on new achievable geometries, which are typical for DfAM practices, are discussed. In Section 3, a case study comprising a heat-treated AM component is presented. In Section 4, the component's hardness is tested, and the effect of heat treatment on its AM features is evaluated and discussed. Last, the study is concluded and further recommendations for designers about thermal post-processing on the PBF-LB of AlSi10Mg parts are summarized.

2. State of the art

2.1. Heat treatments for PBF-LB AlSi10Mg

Thermal post-processing can mitigate residual stresses and diminish anisotropy. Furthermore, it changes mechanical properties like strength and hardness. There are two main ways of heat treatment for AlSi10Mg. On the one hand, to lower residual stresses, low-temperature treatments like annealing or stress relieving at 300 °C for 2h are used (Zhuo et al., 2019). On the other hand, solution heat treatment between 500 °C and 550 °C followed by quenching and artificial aging (T6 heat treatment) can be used to avoid loss in mechanical strength (Fiocchi et al., 2017; Li et al., 2016; Rosenthal et al., 2018). Therefore, for Al-Si-Mg alloys, T6 is the most commonly used heat treatment procedure across several industries. T6 involves three steps: solution annealing, quenching, and natural or artificial aging (Sjölander and Seifeddine, 2010). During solution heat treatment, soluble phases with trace elements like magnesium are dissolved along with homogenization and spheroidisation of the silicon phase (Moustafa et al., 2003). This solutionized phase remains at high temperatures and prevents precipitation of Mg2Si during the quenching process. Then, the additional aging results in homogenous precipitates, which translates into improved strength of the alloy. Aging can be natural, at room temperature, or artificial at temperatures ranging from 150 °C to 210 °C (Zhou et al., 2018). In addition to T6, there are novel thermal post-processing procedures for powder bed fused AlSi10Mg. A good example is the work from Giovagnoli et al. (2021) that developed a new procedure called high-pressure T6 (HPT6). It combines hot isostatic pressing (HIP), quenching in gas, and aging at high pressures. Despite the good results achieved through HPT6, it requires more equipment. A fact that hinders its applicability in some industrial sectors.

https://doi.org/10.1017/pds.2022.62 Published online by Cambridge University Press

2.2. Effect of T6 heat treatment on mechanical properties

The PBF-LB of AlSi10Mg powder can be considered as fast heat treatment, involving solution annealing, quenching, and artificial aging. After fusing each powder layer, fast quenching occurs leading to fine microstructures and preventing the formation of Mg2Si crystals. The result is fine aluminium crystals surrounded by a brittle eutectic structure (Zhou et al., 2018). According to the Hall-Petch strengthening, the material's strength is increased by minimizing the average crystalline grain size, as grain boundaries are a barrier for propagating dislocations. Additionally, when the build platform is pre-heated between 150 °C and 200 °C, artificial aging occurs, giving place to Mg2Si precipitates. The existence of precipitation combined with fine grains in laser powder bed fused AlSi10Mg translates into a high strength, yet a low elongation at break. Additionally, inherent residual stresses and pores, which reduce the fatigue life (Tang and Pistorius, 2017), are typical for PBF-LB processes. In Figure 1, the mechanical properties of conventional manufactured and additive manufactured AlSi10Mg with and without heat treatment are illustrated.

To improve ductility and fatigue life, a T6-like heat treatment is implemented in Section 3.1. The selected T6 heat treatment involves short solution heat treatment, quenching, and artificial aging. As additive manufactured AlSi10Mg already has a fine microstructure, solution heat treatment is only necessary to homogenize the microstructure, reducing anisotropy and therefore homogenizing the mechanical properties. If the solution heat treatment duration extends the optimum, grain coarsening follows, and thus mechanical characteristics like fatigue strength and hardness decrease. As a result of this, thermal post-processing of additive manufactured AlSi10Mg parts should be as long as necessary for homogenisation and as short as possible to avoid further coarsening.

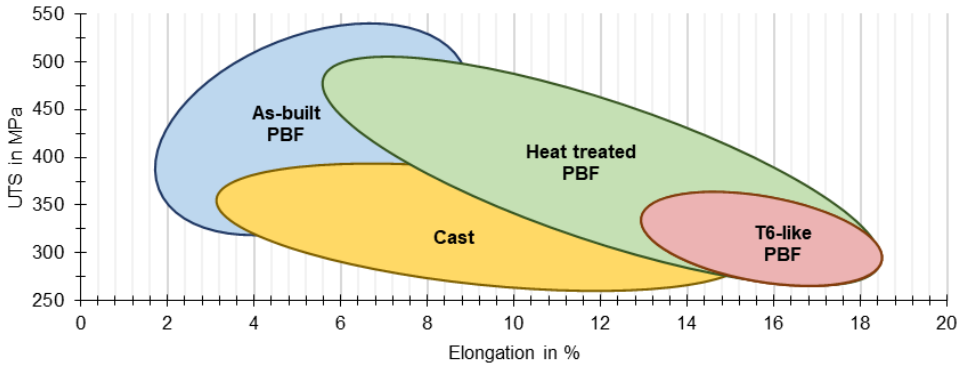

Figure 1. Mechanical properties of AlSi10Mg based on Yan et al. (2020), Wu et al. (2021), Zhang et al. (2021) and Casati et al. (2018)

2.3. Heat-treated mechanical properties of new achievable geometries

The microstructure of PBF-LB parts may differ accordingly to their geometry. This impacts strongly on complex shapes such as lattice structures. Liu et al. (2020a) noted this effect and studied the particular microstructure of additive manufactured AlSi10Mg lattice structures. They reported that a gradient microstructure (a continuous change in microstructure) of primary α-Al bounded by an α-Al/Si eutectic phase develops in the major structural sections of the lattice, e.g. the nodes. In the upper part of the lattice nodes, columnar α-Al phases were observed. In the bottom part of the nodes, coarser and more equiaxed α-Al phases were found. This is an effect of the different cooling rates of the nodes section. The lower part of the nodes is built as unsupported regions on the powder bed, which affects thermal conductivity. As a result, lower hardness was reported on the lower sections, i.e. the coarsened regions. As discussed in the previous section, the effect of heat treatment on mechanical properties was extensively studied. Usually, these results are reported for the bulk, i.e., for solid material tested from standardised test specimens. Still, results are different for complex structures, which are achieved by the means of AM. After printing, parts might exhibit a complex residual stress state. As it is impossible to know, if any of the stress tensor components are close to failure, thermal post-processing is performed right away to relieve the part from stresses. This means the part undergoes heat treatment including the support structure and likely with entrapped powder in cavities. The presence of complex shapes and

https://doi.org/10.1017/pds.2022.62 Published online by Cambridge University Press

barriers, such as powder or support structure, might affect the thermal gradients during heat treatment, and consequently, its effect on the mechanical properties. Therefore, as heat treatment effects depend on heat gradients determined by the part's geometry and the alloy's thermal properties, it is not feasible to obtain generic results that apply to complex components. For that reason, Liu et al. (2020b) analysed the effect of solution heat treatments on lattice structures. To investigate the areas where heat treatment had an impact, they measured the hardness on different lattice sections within a simple test specimen. Liu et al. (2020b) reported that solution heat treatment at 530 °C is necessary to achieve a resulting microstructure consisting of a primary α-Al phase with coarsened Si particles and a stable Fe-containing intermetallic phase (β-AlFeSi) at all locations of the lattice structure. The resulting homogeneity leads to constant hardness across the whole lattice structure. Still, the hardness values are lower than in the as-built condition due to grain coarsening. However, their specimen was simple, free of support structures or entrapped powder, and far from a geometry that may be found in an industrial component.

3. Materials and methods

3.1. Manufacturing setup

The AlSi10Mg part, which is evaluated in this study, was fabricated using an SLM®125 PBF-LB machine. The scanning speed for hatching was set to 1650 mm/s at a laser power of 350 W with a layer thickness of 30 µm. The slicing stripe width was 10 mm with a hatch spacing of 130 µm. A rotating scan pattern was used with a layer rotation angle of 67°, starting at 0° for the initial layer. The base plate was preheated to a temperature of 150 °C. Commercially available AlSi10Mg powder of the manufacturer SLM Solutions with a particle size between 20 µm and 63 µm was used in this case. The manufactured part is an experimental piston, intended to be used as a spare part for a Ford V8 292 Y-Block engine. The piston was designed following the spare part design methodology developed by Montero and Weber et al. (2020). The section, which serves as a structure to connect the pin boss with the piston head (see. Figure 4-1), was topological optimised to resist a cyclic load at a reduced volume and a pre-determined centre of mass. Furthermore, the structure contains a lattice structure (see. Figure 4-2), as the increased complexity comes at no additional manufacturing expanse. As it was of importance for the designers to obtain a clean as-printed surface on the piston's head, the piston was printed in an upright position. This required additional support structure on the inside (see. Figure 2 left). The support structure was designed as tree-like support for better heat dissipation. These design characteristics point out the suitability of the piston as an experimental part to expose the effects of heat treatment on unconventional, but typical AM features, such as topological optimised surfaces and lattice structures. A picture of the printed piston is presented in Figure 2 on the right.

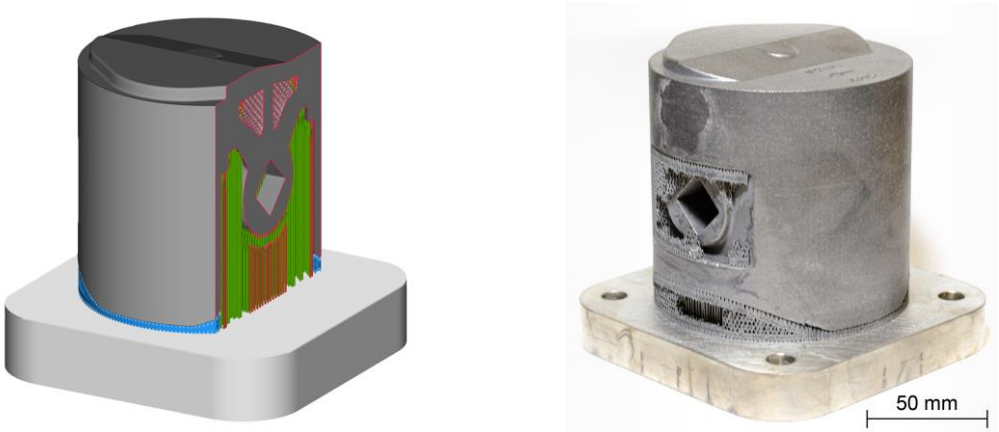

Figure 2. Build job including a support structure. Build preparation (left) and manufactured part in as-built condition (right).

To resemble typical industrial conditions, the post-processing involved a T6-like treatment and manual support removal. The heat treatment was performed in an air-circulating furnace N 30/85HA

https://doi.org/10.1017/pds.2022.62 Published online by Cambridge University Press

(Nabertherm GmbH, Germany) within an uncontrolled atmosphere including oxygen. The heat treatment ended with quenching of the part in water, down to 25 °C. The temperature vs. time graph is shown in Figure 3. Both thermal elements, which were used to monitor the temperature of the furnace and the piston, were placed at each centre. Following the solution treatment, artificial aging was performed for 6 hours at 165 °C.

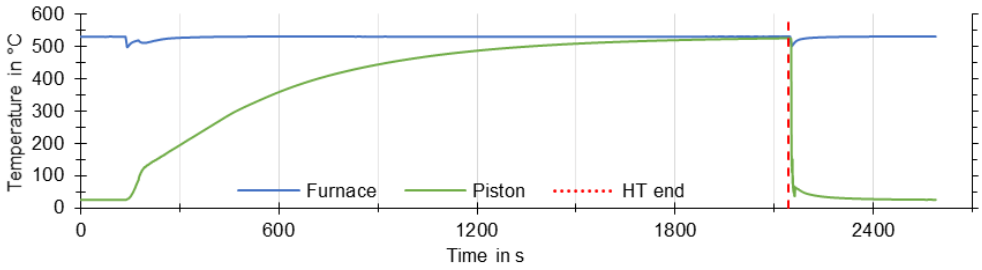

Figure 3. Heat treatment temperature curve of the piston

3.2. Testing setup

To evaluate the effect of heat treatment on the hardness of AlSi10Mg components, Vickers hardness tests according to DIN EN ISO 6507-1 were performed. The hardness of the additive manufactured piston was measured in HV 1, using a testing machine of the type KB 250 (KB Prüftechnik GmbH, Germany). Before any measurements were taken, the piston was cut into several slices (see. Figure 4, Figure 5, and Figure 6), which were subsequently polished using the polishing machine AutoMet™ 950 (Bühler Holding AG, Switzerland). In Figure 4, the topology optimised section (1) of the piston can be observed and the internal lattice structure (2) is exposed. The measurement positions A through J are displayed along with the measurement direction as dotted arrows in Figure 5 and Figure 6.

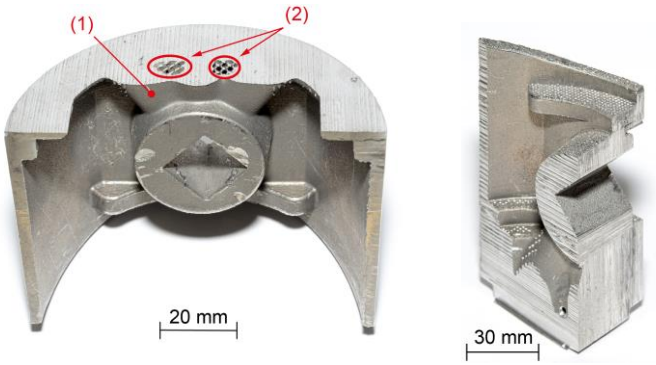

Figure 4. Half section-cut of the piston with piston head removed (left) with (1) topology optimised section and (2) lattice structure. Cut through the non-machined pin bore (right).

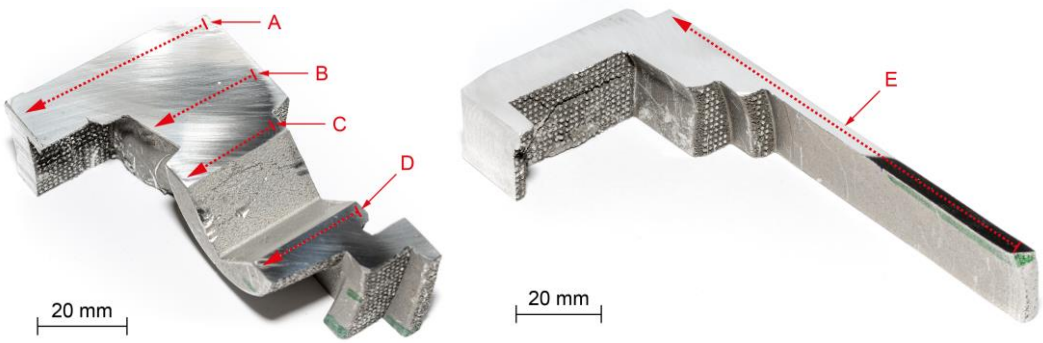

Figure 5. Slice through the non-machined pin bore with measurement positions A-D (left) and perpendicular slice with measurement position E (right)

https://doi.org/10.1017/pds.2022.62 Published online by Cambridge University Press

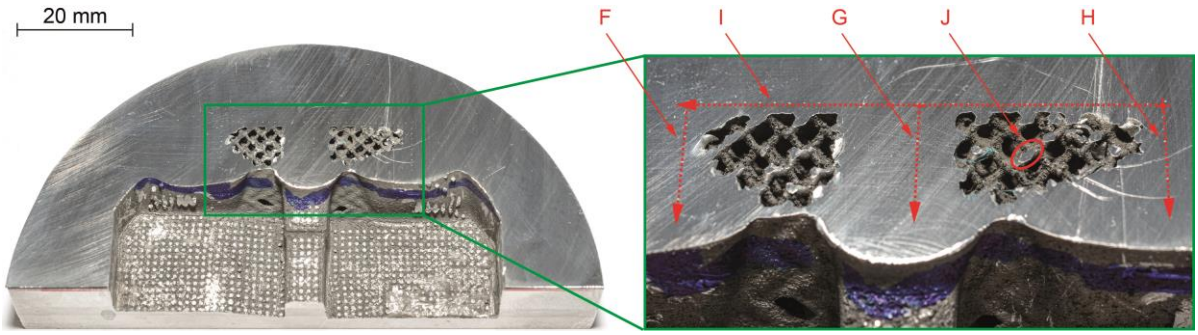

Figure 6. A bottom-up view of the piston head with measurement positions F-J and a detailed view of the internal lattice structure

4. Results and discussion

Several measurements were taken at different locations of the piston, as described in the previous section. The resulting hardness profiles with data values in HV 1 are presented in Figure 7. The first group of measurements (profile A) was taken at the piston head, starting from the outside surface towards the centre of the piston with a length of 40 mm. The HV 1 hardness was in the range of 91.3 HV 1 and 106 HV 1. The measured values decreased slightly from the outside (103 HV 1) towards the inside (96.4 HV1) of the piston. Similar behaviour was detected for a wall thickness of approximately 25 mm for the profiles B, C, and D. The measured hardness for these sections was in the range of 104 HV 1 and 89.6 HV 1 with 103 HV 1 at the start of profile B, and 101 HV 1 and 100 HV 1 for the profiles C and D respectively. For the inner end of these profiles, values of 93.8 HV 1 (B), 93.2 HV 1 (C), and 91.8 HV 1 (D) were obtained. The consistency between the values of the three different profiles implies no effect of the topology optimised section on the heat treatment process or the hardness, respectively. The decrease of hardness towards the inside of the piston on the other hand shows the influence of the wall thickness on the heat treatment. The heat conduction during the heating phase of the heat treatment as well as the quenching process is affected by thicker sections of the part. Majeed et al. (2019) also detected a significant influence of the part's wall thickness on hardness after heat treatment. In their study, the hardness varied between 137.3 HV and 102.4 HV, dependent on the wall thickness. Similar results for the hardness of solution heat-treated cubic samples were gathered by Aboulkhair et al. (2016). High hardness values can be achieved by forming fine and small grain structures, which can be further obtained by appropriate heat treatment (Hall-Petch strengthening) with subsequent quenching. The faster the quenching is performed, the fewer changes in microstructure occur. Keeping this effect in mind, the hardness differences between the inside and the outside of the piston might result from inhomogeneous quenching.

Profile E shows the measured hardness across the piston skirt. With values between 96 HV 1 and 103 HV 1, this section is considerably more homogeneous than the others are. This implies that the support structure next to this section on the inside of the piston had no significant effect on the T6-like heat treatment and the quenching process. The single hardness value of 109 HV 1 at 70 mm of profile E was considered to be an outlier and therefore not further evaluated. One possible reason for this might be a harder Si-structure that was located at this measurement position as the result of inhomogeneous material due to the varying wall thickness of the piston. With hardness values of profile E being in a similar range as the outside values of the profiles A - D, it is inferred that the position on the build plate has no significant effect on the heat treatment, as well as the quenching, and therefore also on the hardness.

The hardness results of the topology optimised structure, which is partly visible in Figure 5 and evaluated in the profiles F-I, showed a promising homogeneity, despite the large wall thickness. The lattice structure, which is used to fill gaps in the piston's design, connects solid structures and leads to less variation in hardness compared to the profiles A - E. The tangential profile I showed a variation in hardness between 94.1 HV 1 and 112 HV 1. For the profiles F, G and H, hardness extrema were measured as 102 HV 1 and 113 HV 1 for profile F, 94 HV 1 and 105 HV 1 for profile G, and 100 HV 1 and 108 HV 1 for profile C. The minimum hardness at G after 4 mm was not evaluated in detail and

https://doi.org/10.1017/pds.2022.62 Published online by Cambridge University Press

considered as an outlier. It is expected that this significantly lower value is caused by a process-induced pore at the place of the hardness measurement. Furthermore, the tree-like support structure and its placement act beneficial on the infiltrating of the water, and therefore fast quenching may be endorsed. Liu et al. (2020b) determined that lattice structures lead to a homogeneous hardness due to improved heat transfer to the cooling medium. The samples evaluated in this work benefit from that improved heat dissipation. Measurements next to the lattice structure led to a similar hardness than measurements on the outside of the piston. Therefore, the utilization of lattice structures in parts with high wall thicknesses has a beneficial effect on thermal dissipation, which further results in a homogenous increase of hardness. For the lattice structure itself (measurement position J), six individual measurements were taken at different locations of the lattice structure. The evaluated hardness was between 92.2 HV 1 and 102 HV 1. One single measurement resulted in a Vickers hardness of 83.3 HV 1, which is considered an outlier. This reduced value might result from a pore, which was located at the measurement position.

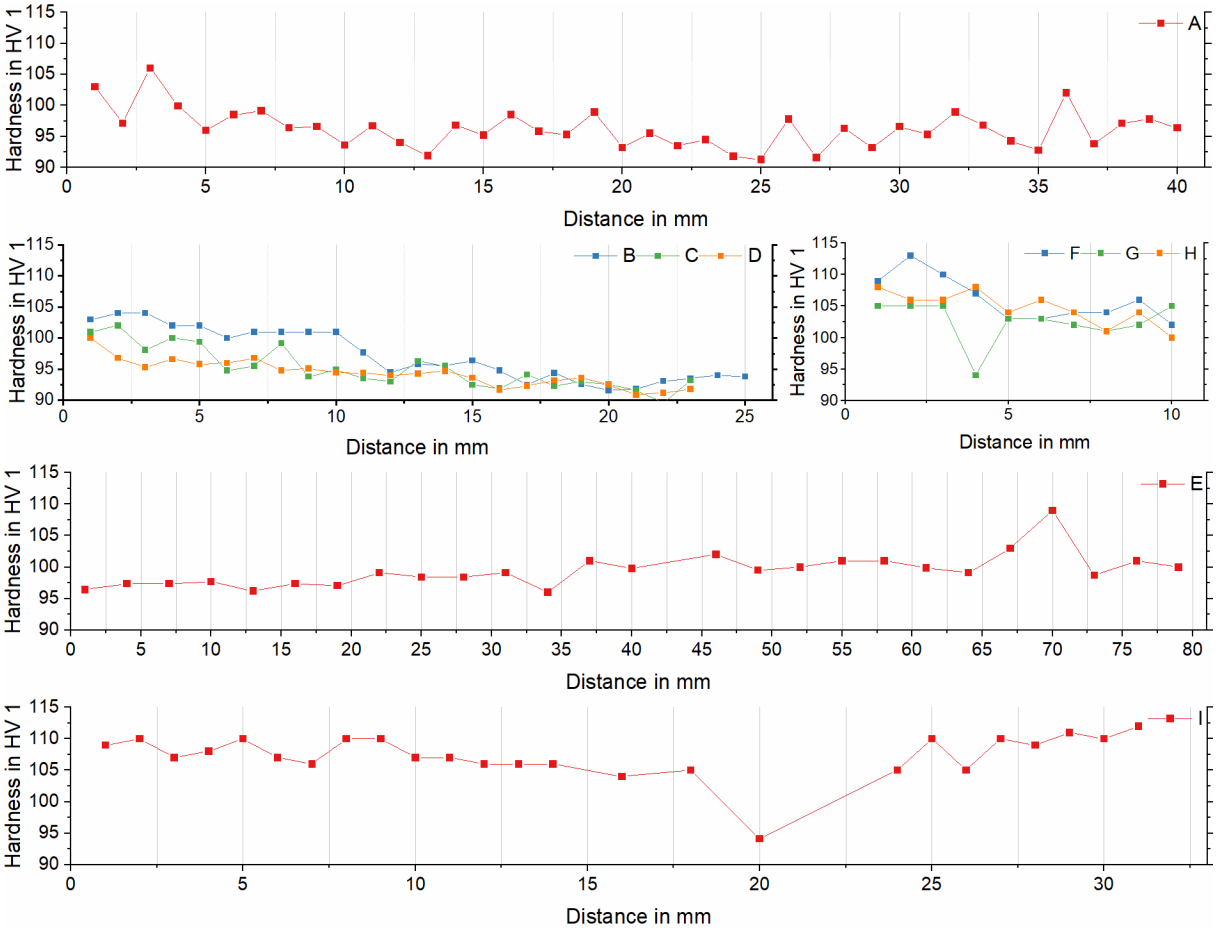

Figure 7. Hardness Measurements (HV 1) for A - I

5. Conclusions

This article analysed the effect of heat treatment for unconventional geometries achievable by metal AM processes. Thermal post-processing is essential for laser powder bed fused AlSi10Mg parts to improve their tenacity and toughness, particularly for those components designed for high load conditions. The homogeneity-related issues are the most influential factor in performance evaluation, and complex geometries may enhance inhomogeneity in the PBF-LB parts. To tackle the RQ1 stated in the introduction, the investigation on the industrial component showed that the T6-like heat treatment reached good, yet not optimal homogeneity reflected as a gradient on the hardness profiles across the tested surfaces. The reason is that the part had inner cavities that were not thoroughly reachable by the cooling agent (water) and its large cross-sections. That is a usual situation for optimised components.

https://doi.org/10.1017/pds.2022.62 Published online by Cambridge University Press

In addition, components printed by PBF-LB need a support structure that may act as a barrier for heat treatment, particularly the quenching. Furthermore, DfAM encourages designers to exploit complex shapes such as topology optimised surfaces and lattice structures. This could represent a barrier to optimal heat treatment due to the requirement of the extra support structure. Additionally, lattice structures are sometimes closed by a shell with a hole for powder extraction, impeding the infiltration by the cooling medium. Although this might affect the heat treatment within the lattice, the investigated part showed slightly lower values (92.2 HV 1 - 102 HV 1) compared to the surfaces in direct contact with the cooling medium. Moreover, it was observed that the part's wall thickness influenced the quenching. The hardness values decreased as the wall thickness increased, as thermal conduction plays a role for thicker cross-sections. Outer surfaces showed peaks of around 105 HV 1, which dropped to approximately 90 HV 1 as the measurements advanced towards the centre of the part. As a remark, hardness values in the regions in contact with the inner lattice, e.g. profile I and G, were comparable to the peaks of the outer surfaces, highlighting the beneficial effect of heat dissipation generated by the lattice.

As a consequence, and to tackle RQ2, if thermal post-processing is performed on additive manufactured AlSi10Mg parts, the following additions to the DfAM knowledge base are recommended for designers:

- Design the build using a tree-like support structure or pin-support to avoid barriers for heat transfer, especially for quenching.
- Bear in mind that large cross-sections diminish the effect of heat treatment, especially for quenching. This should be considered particularly for topology optimised bodies, which might have large cross-sections next to the loaded faces. Further, complex shapes resulting from optimisations may require additional support structures that might act as a barrier for heat treatment.
- Lattice structures can reach homogeneous properties after solution heat treatment over 500 °C. If quenching is performed, the cooling medium has to infiltrate the inner lattice properly.
- The hardness values in the outer faces of the part were similar to the hardness values in the large cross-section, which were in contact with the lattice structure. This demonstrates the ability of the lattice structure to dissipate heat during quenching.
- It is possible to apply T6-like heat treatment to shell-lattices (fully enclosed lattices), as the cooling medium reaches the inside via the depowdering holes. The heat transfer is comparable or likely better than for a solid section, which was confirmed for dimensions of the lattice structure of approximately 10 mm to 15 mm.

Future research could investigate the effect of various materials on the measured hardness, as different materials require other heat treatment profiles. In addition, other complex geometries might be evaluated for the aim of providing quantitative correlations between design parameters and the heat treatment effect.

Acknowledgments

This work was partially funded by *dtec.bw* and is part of the project *FLAB-3DPRINT*.

References

Aboulkhair, N.T., Maskery, I., Tuck, C., Ashcroft, I. and Everitt, N.M. (2016), "The microstructure and mechanical properties of selectively laser melted AlSi10Mg: The effect of a conventional T6-like heat treatment", Materials Science and Engineering: A, Vol. 667, pp. 139–146, https://doi.org/10.1016/j.msea.2016.04.092.

Brackett, D., Ashcroft, I. and Hague, R. (2011), "Topology optimization for additive manufacturing", 2011 International Solid Freeform Fabrication Symposium, University of Texas at Austin.

Casati, R., Hamidi Nasab, M., Coduri, M., Tirelli, V. and Vedani, M. (2018), "Effects of Platform Pre-Heating and Thermal-Treatment Strategies on Properties of AlSi10Mg Alloy Processed by Selective Laser Melting", Metals, Vol. 8 No. 11, p. 954, https://doi.org/10.3390/met8110954.

Cheng, L., Liang, X., Bai, J., Chen, Q., Lemon, J. and To, A. (2019), "On utilizing topology optimization to design support structure to prevent residual stress induced build failure in laser powder bed metal additive manufacturing", Additive Manufacturing, Elsevier, Vol. 27, pp. 290–304.

https://doi.org/10.1017/pds.2022.62 Published online by Cambridge University Press

Cloots, M., Spierings, A. and Wegener, K. (2013), "Assessing new support minimizing strategies for the additive manufacturing technology SLM", Solid Freeform Fabrication Symposium (SFF), Austin, TX, pp. 12–14.
Fiocchi, J., Tuissi, A., Bassani, P. and Biffi, C.A. (2017), "Low temperature annealing dedicated to AlSi10Mg selective laser melting products", Journal of Alloys and Compounds, Vol. 695, pp. 3402–3409, https://doi.org/10.1016/j.jallcom.2016.12.019.
Giovagnoli, M., Tocci, M., Fortini, A., Merlin, M., Ferroni, M., Migliori, A. and Pola, A. (2021), "Effect of different heat-treatment routes on the impact properties of an additively manufactured AlSi10Mg alloy", Materials Science and Engineering: A, Vol. 802, p. 140671, https://doi.org/10.1016/j.msea.2020.140671.
Kirchheim, A., Dennig, H.-J. and Zumofen, L. (2017), "Why education and training in the field of additive manufacturing is a necessity", International Conference on Additive Manufacturing in Products and Applications, Springer, pp. 329–336.
Kok, Y., Tan, X.P., Wang, P., Nai, M.L.S., Loh, N.H., Liu, E. and Tor, S.B. (2018), "Anisotropy and heterogeneity of microstructure and mechanical properties in metal additive manufacturing: A critical review", Materials & Design, Vol. 139, pp. 565–586, https://doi.org/10.1016/j.matdes.2017.11.021.
Li, W., Li, S., Liu, J., Zhang, A., Zhou, Y., Wei, Q., Yan, C., et al. (2016), "Effect of heat treatment on AlSi10Mg alloy fabricated by selective laser melting: Microstructure evolution, mechanical properties and fracture mechanism", Materials Science and Engineering: A, Vol. 663, pp. 116–125, https://doi.org/10.1016/j.msea.2016.03.088.
Liu, M., Takata, N., Suzuki, A. and Kobashi, M. (2020a), "Development of gradient microstructure in the lattice structure of AlSi10Mg alloy fabricated by selective laser melting", Journal of Materials Science & Technology, Vol. 36, pp. 106–117, https://doi.org/10.1016/j.jmst.2019.06.015.
Liu, M., Takata, N., Suzuki, A. and Kobashi, M. (2020b), "Effect of Heat Treatment on Gradient Microstructure of AlSi10Mg Lattice Structure Manufactured by Laser Powder Bed Fusion", Materials, Vol. 13 No. 11, p. 2487, https://doi.org/10.3390/ma13112487.
Majeed, A., Lv, J., Zhang, Y., Muzamil, M., Waqas, A., Shamim, K., Qureshi, M.E., et al. (2019), "An investigation into the influence of processing parameters on the surface quality of AlSi10Mg parts by SLM process", 2019 16th International Bhurban Conference on Applied Sciences and Technology (IBCAST), presented at the 2019 16th International Bhurban Conference on Applied Sciences and Technology (IBCAST - 2019), IEEE, Islamabad, Pakistan, pp. 143–147, https://doi.org/10.1109/IBCAST.2019.8667175.
Montero, J., Weber, S., Bleckmann, M. and Paetzold, K. (2020), "A methodology for the decentralised design and production of additive manufactured spare parts", Production & Manufacturing Research, Vol. 8 No. 1, pp. 313–334, https://doi.org/10.1080/21693277.2020.1790437.
Moustafa, M.A., Samuel, F.H. and Doty, H.W. (2003), "Effect of solution heat treatment and additives on the microstructure of Al-Si (A413.1) automotive alloys", Journal of Materials Science, Vol. 38 No. 22, pp. 4507–4522, https://doi.org/10.1023/A:1027333602276.
Read, N., Wang, W., Essa, K. and Attallah, M.M. (2015), "Selective laser melting of AlSi10Mg alloy: Process optimisation and mechanical properties development", Materials & Design (1980-2015), Vol. 65, pp. 417–424, https://doi.org/10.1016/j.matdes.2014.09.044.
Rosenthal, I., Shneck, R. and Stern, A. (2018), "Heat treatment effect on the mechanical properties and fracture mechanism in AlSi10Mg fabricated by additive manufacturing selective laser melting process", Materials Science and Engineering: A, Vol. 729, pp. 310–322, https://doi.org/10.1016/j.msea.2018.05.074.
Schmitt, M., Kempter, B., Schlick, G. and Reinhart, G. (2020), "Parameter identification approach for support structures in laser powder bed fusion and analysis of influencing factors", Procedia CIRP, Vol. 94, pp. 260–265, https://doi.org/10.1016/j.procir.2020.09.049.
Schuch, M., Hahn, T. and Bleckmann, M. (2021), "The mechanical behavior and microstructure of additively manufactured AlSi10Mg for different material states and loading conditions", Materials Science and Engineering: A, Vol. 813, p. 141134, https://doi.org/10.1016/j.msea.2021.141134.
Sjölander, E. and Seifeddine, S. (2010), "The heat treatment of Al–Si–Cu–Mg casting alloys", Journal of Materials Processing Technology, Vol. 210 No. 10, pp. 1249–1259, https://doi.org/10.1016/j.jmatprotec.2010.03.020.
Tang, M. and Pistorius, P.C. (2017), "Oxides, porosity and fatigue performance of AlSi10Mg parts produced by selective laser melting", International Journal of Fatigue, Elsevier, Vol. 94, pp. 192–201.
Thompson, M.K., Moroni, G., Vaneker, T., Fadel, G., Campbell, R.I., Gibson, I., Bernard, A., et al. (2016), "Design for Additive Manufacturing: Trends, opportunities, considerations, and constraints", CIRP Annals, Vol. 65 No. 2, pp. 737–760, https://doi.org/10.1016/j.cirp.2016.05.004.
Vaneker, T., Bernard, A., Moroni, G., Gibson, I. and Zhang, Y. (2020), "Design for additive manufacturing: Framework and methodology", CIRP Annals, Elsevier, Vol. 69 No. 2, pp. 578–599.
Wu, H., Ren, Y., Ren, J., Liang, L., Li, R., Fang, Q., Cai, A., et al. (2021), "Selective laser melted AlSi10Mg alloy under melting mode transition: Microstructure evolution, nanomechanical behaviors and tensile properties", Journal of Alloys and Compounds, Vol. 873, p. 159823, https://doi.org/10.1016/j.jallcom.2021.159823.

https://doi.org/10.1017/pds.2022.62 Published online by Cambridge University Press

Yan, Q., Song, B. and Shi, Y. (2020), "Comparative study of performance comparison of AlSi10Mg alloy prepared by selective laser melting and casting", Journal of Materials Science & Technology, Vol. 41, pp. 199–208, https://doi.org/10.1016/j.jmst.2019.08.049.

Zhang, X.X., Lutz, A., Andrä, H., Lahres, M., Gan, W.M., Maawad, E. and Emmelmann, C. (2021), "Evolution of microscopic strains, stresses, and dislocation density during in-situ tensile loading of additively manufactured AlSi10Mg alloy", International Journal of Plasticity, Vol. 139, p. 102946, https://doi.org/10.1016/j.ijplas.2021.102946.

Zhou, L., Mehta, A., Schulz, E., McWilliams, B., Cho, K. and Sohn, Y. (2018), "Microstructure, precipitates and hardness of selectively laser melted AlSi10Mg alloy before and after heat treatment", Materials Characterization, Vol. 143, pp. 5–17, https://doi.org/10.1016/j.matchar.2018.04.022.

Zhuo, L., Wang, Z., Zhang, H., Yin, E., Wang, Y., Xu, T. and Li, C. (2019), "Effect of post-process heat treatment on microstructure and properties of selective laser melted AlSi10Mg alloy", Materials Letters, Vol. 234, pp. 196–200, https://doi.org/10.1016/j.matlet.2018.09.109.

https://doi.org/10.1017/pds.2022.62 Published online by Cambridge University Press